

Depth-resolved imaging of nematic liquid crystals by third-harmonic microscopy

D. Yelin and Y. Silberberg^{a)}

Department of Physics of Complex Systems, Weizmann Institute of Science, Rehovot 76100, Israel

Y. Barad and J. S. Patel

Department of Physics, Pennsylvania State University, University Park, Pennsylvania 16802

(Received 5 January 1999; accepted for publication 30 March 1999)

Third-harmonic microscopy is shown to be a powerful tool for the study of liquid crystal structures. The third-harmonic probe enables the investigation of molecular order well inside a liquid crystal cell. The observation of phase transition in various nematic liquid crystal samples is presented as a demonstration for the power of this technique. For example, nematic and isotropic regions are shown to coexist across the depth of the cell. Thermal fluctuations are observed in the nematic regions close to the isotropic–nematic transition temperature. © 1999 American Institute of Physics. [S0003-6951(99)04321-1]

Third-harmonic generation scanning laser microscopy has been shown to be a powerful tool for the investigation of transparent materials, as it can produce three-dimensional images of such samples.^{1,2} In this letter, we show that when applied to liquid crystalline materials, third-harmonic microscopy can yield important information on molecular orientation within the samples. Thereby, we observed a rich variety of phenomena, ranging from simple domain formation to growth dynamics.

The study of liquid crystalline materials is important because the last decades have seen impressive advances in applications of these materials³ that require detailed understanding of their structures.⁴ An important aspect of liquid crystal (LC) research is the knowledge of the three-dimensional ordering of the molecules within LC cells.⁵ This is most commonly done using electromagnetic radiation, in the visible and the x-ray regions of the spectrum.⁶ However, in most cases the three-dimensional structure is difficult to obtain, particularly in thin cells. We show that by using third-harmonic microscopy it is possible to obtain information on molecular order in the depth of the liquid crystal cell.

Third-harmonic generation (THG) microscopy is a form of laser scanning microscopy, where third-harmonic light is generated near the focal point of a tightly focused femtosecond laser beam. This technique allows improved contrast over standard phase microscopy, with the additional advantage of depth resolution. A tightly focused Gaussian beam in a homogeneous medium results in zero THG.⁷ Only variations in the nonlinear optical properties of the medium, specifically the third-order susceptibility $\chi^{(3)}$, result in THG. In liquid crystals, the relevant component of $\chi^{(3)}$ depends on the relation between the direction of the optical field and the molecular orientation, and therefore THG microscopy can give valuable information on the internal structure of the LC sample. Other scanning laser techniques have been applied to LC research. A study of the internal texture of a polymer-stabilized cholesteric LC using linear confocal microscopy,

based on fluorescence from the polymer network^{8,9} and by detecting the light scattered by disordered regions within the LC,⁹ was recently reported. The advantage of THG microscopy is that it probes the molecular orientation and the order at the focal plane without the need for any additional markers. The nonlinearity enhances the sensitivity of the method as well as its depth resolution, as compared with linear laser scanning methods.

Phase transitions in nematic LCs has fascinated researchers since the early days of the field.¹⁰ At high temperatures, the LC is an isotropic, homogeneous liquid. The isotropic–nematic (I–N) phase transition occurs at some critical temperature T_c . Below T_c the LC gains a long distance orientational order and becomes birefringent.

In the following we report an experiment which resolves the crystallization (nucleation) process of a liquid crystal layer, along the depth of the cell, from the isotropic liquid to the nematic phase. The experimental setup used is shown in Fig. 1. The laser source is a synchronously pumped OPO

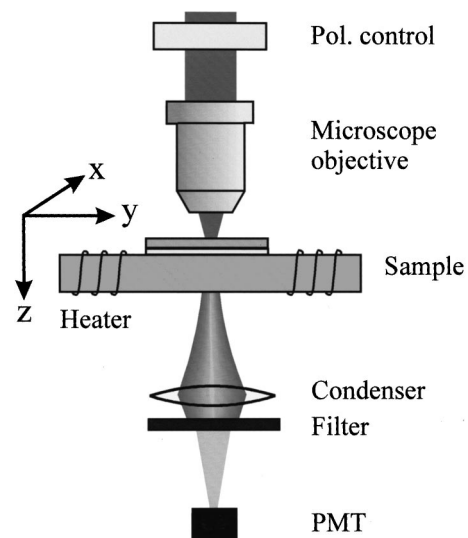


FIG. 1. A schematic description of the experimental setup for THG microscopy of liquid crystal samples.

^{a)}Electronic mail: feyaron@wis.weizmann.ac.il

(spectra-physics tsunami-opal system) which provides 130 fs pulses at a wavelength of $1.5 \mu\text{m}$ at a repetition rate of 80 MHz. The laser beam is focused into the LC sample at normal incidence, using a $\times 60$, $\text{NA}=0.85$ microscope objective. The LC sample is scanned in the z direction using a piezoelectric driven stage. The third-harmonic light at the wavelength of $0.5 \mu\text{m}$ is collected by a lens and measured by a photomultiplier tube (PMT) after filtering out the fundamental wavelength. The polarization and the power of the injected beam is controlled using an attenuator, a polarizer and a $\lambda/2$ plate. Two LC samples were used in the experiment: a nematic cell and a twisted nematic cell. Both samples were $50 \mu\text{m}$ thick and filled with E7 LC. Each cell had a small heater attached to the bottom glass, in order to control the cell temperature. A small temperature gradient is thus formed between the top and bottom glass plates. The coordinate frame is chosen so that the cover glass–LC interface is in the x - y plane while the rubbing direction at this plane is along the y axis. The electromagnetic field therefore propagates along the positive z axis. The focal point of the laser beam is scanned along the z axis at a repetition rate of one line per second. The average laser power in these measurements was kept low (5 mW) in order to avoid laser induced thermal or molecular orientation changes. To verify that the laser irradiation does not affect the sample through heating or other processes, we repeated the measurements at various laser powers and at different scan rates. It was determined that the results were independent of those parameters at our working conditions. At significantly higher laser powers, above ~ 30 mW of average power, the measurements started to deviate from those obtained at low powers. We believe that the main reason for these deviations is laser-induced molecular reorientation.

In the first set of measurements, we made dynamic and quasiequilibrium studies of a linearly aligned nematic LC near its I–N phase transition point. In the dynamic studies, the LC sample was scanned as it was slowly cooled across the phase transition point [Figs. 2(a) and 2(c)]. In the quasistatic measurements, the temperature was stabilized close to the I–N phase transition point [Figs. 2(b) and 2(d)]. The polarization of the light was either along the alignment direction [Figs. 2(a) and 2(b)] or perpendicular to it [Figs. 2(c) and 2(d)]. Each image is composed of 200 line scans along the z axis, at the same (x,y) location. The third harmonic power is represented in a grey scale, normalized to the strongest signal in each set. Darker grey represents higher THG power.

Consider first the dynamic study of Fig. 2(a), where the light is polarized along the rubbing direction (y axis). As long as the cell is at a temperature higher than T_c , the LC is completely isotropic and only the glass–LC interfaces at $z=0$ and $z=50 \mu\text{m}$ generate third-harmonic light, as expected. After a few scans, the top of the sample cools below T_c , and a strong increase of THG is observed. This strong signal is caused by the large third-order susceptibility of the ordered phase when the molecules begin to arrange with their long axis parallel to the rubbing direction, which is the direction of optical field. These measurements indicate that

$$\chi_{yyyy}^{\text{LC}} \approx 8\chi_{1111}^{\text{glass}}, \quad (1)$$

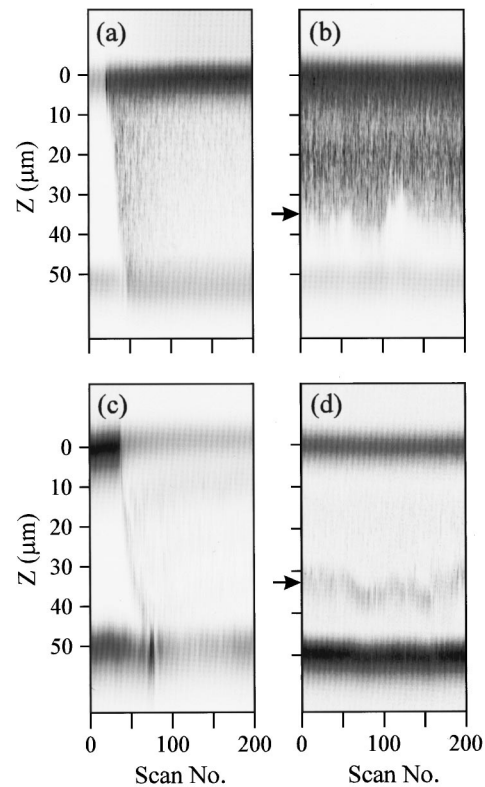


FIG. 2. Imaging of the I–N phase transition in a parallel nematic LC cell. Each image is composed of a set of 200 scans of a tightly focused laser beam along the z axis. THG power is represented in a gray scale normalized to the strongest signal in each set, where high powers are dark. The first two sets were taken during the cooling of the sample (a), and at a stable temperature gradient around T_c (b), both with light polarized along the y axis (the rubbing direction). The images (c) and (d) were taken under the same conditions as in (a) and (b), respectively, using light polarized along the x axis. The nematic and the isotropic phases are clearly observed simultaneously along the depth of the sample in sets (b) and (d). Arrows mark the interface between these layers.

and

$$\chi_{xxxx}^{\text{LC}} \approx \chi_{1111}^{\text{glass}}, \quad (2)$$

where χ_{xxxx}^{LC} and χ_{yyyy}^{LC} are the third-order susceptibility tensor components of the LC along the x and the y directions, respectively, and $\chi_{1111}^{\text{glass}}$ is the relevant tensor component of the glass substrate, where the index 1 may stand for any direction.

Due to the temperature gradient imposed on the cell, the I–N phase transition is not expected to occur simultaneously over the sample depth, but rather to begin at the cooler interface. We observe a front of ordered nematic phase that propagates from the top to the bottom of the cell, as can be seen between the twentieth and the fiftieth scans. In these scans, the top region closer to the cooler cover glass is at a temperature slightly below T_c and is therefore in the nematic phase. Being close to the phase transition temperature, this region has a finite amount of order with considerably large thermal fluctuations. The bottom region remains isotropic up to the fiftieth scan, after which the nematic phase takes over the entire sample.

Coexistence of the nematic and the isotropic phases within the LC sample was achieved by stabilizing the temperature gradient close to T_c . A set of scans at a constant temperature gradient is shown in Fig. 2(b). The I–N interface

is clearly seen inside the cell around $z \approx 35 \mu\text{m}$ (indicated by a small arrow in the figure). A slow movement of this boundary layer, with a characteristic time of a few seconds, can be seen. This dynamics of the crystallization-melting front is possibly due to temperature fluctuations. A remarkable feature in Fig. 2(b) is that strong third-harmonic light is generated throughout the entire nematic region. Since THG is not expected in homogeneous regions of the sample, we conclude that the nematic phase exhibits strong thermal fluctuations. Moreover, to explain the observed signal, the size of these fluctuations must be comparable to the focal depth, a few microns in our experiment. Indeed, fluctuations in the molecular alignment are expected near T_c , which lead to decrease of molecular order. We note that consecutive scans produce different distributions of THG, which suggests that the typical correlation time is considerably shorter than 1 s. As the temperature decreases the thermal fluctuations also decrease leading to lower THG from the LC as it becomes more and more homogeneous. This can be seen in the last scans in Fig. 2(a). As the sample cools further, the THG signal from within the nematic LC completely vanishes.

These dynamic and quasiequilibrium measurements were repeated with the light polarized along the x axis [Figs. 2(c) and 2(d)]. In contrast to Fig. 2(a), Fig. 2(c) exhibits a sudden drop of the THG signal at the interfaces on the I–N transition. This is because the relevant third-order susceptibility tensor component of the LC is nearly identical to that of the glass substrate, leading to only small THG at the interface. Juxtaposing Figs. 2(b) and 2(d), it is evident that the strong fluctuations from the nematic region are not visible with light polarized along the x direction, probably because of the relatively small value of the relevant susceptibility term. Because the THG from the nematic region is relatively weak, the THG from the boundary layer between the nematic and the isotropic phases is clearly visible.

We have applied the same imaging technique to study the I–N phase transition in a twisted nematic cell. In this sample, the bottom substrate is rubbed along the x axis, while the top substrate is rubbed along the y axis. When the LC is in the nematic phase, this configuration forms a twisted structure, with the director of the LC molecules pointing along the y axis at the top interface and is gradually rotating to lay along the x axis at the bottom. The Mauguin limit¹⁰ is satisfied in this sample, therefore light injected into the sample, polarized along the y axis, will emerge from the sample polarized along the x axis. THG imaging of a twisted nematic cell, cooling across the I–N phase transition, is shown in Fig. 3(a). As previously, we see the growth of a nematic region, aligned in the y direction, toward the bottom of the cell. Simultaneously, we observe a significant decrease of the THG signal at the bottom interface. The LC layer growing from the top has no twist since the bottom alignment layer has not yet affected it. The light polarization remains unaltered as it reaches the thin layer of molecules, pointing in the x direction, which has already formed at the bottom interface. This leads to the lower THG signal at the bottom. When the twisted nematic configuration is suddenly formed (at the sixtieth scan), the light polarization rotates abruptly with the twisted structure, and the THG at the back interface abruptly increases and remains almost constant.

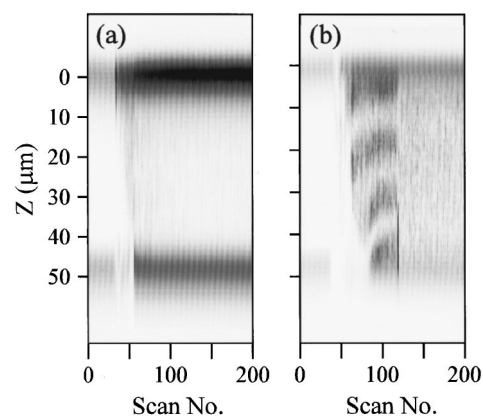


FIG. 3. (a) Set of scans taken during a cooling process of a twisted nematic LC sample; (b) a periodic metastable structure is formed during a phase transition in a simple parallel nematic cell, which abruptly decays to a normal nematic phase with thermal fluctuations.

Various metastable configurations could be observed when the samples were cooled at a relatively fast rate. For example, Fig. 3(b) shows an image obtained after fast cooling of a parallel nematic cell through the I–N phase transition temperature. The light is polarized along the rubbing direction. A periodic structure of unclear origin is formed at the I–N transition, abruptly decaying after a few seconds (at the 120th scan) to the normal nematic structure. This structure was obtained in several measurements, and was just one of a few metastable configurations that were observed in various types of cells.

In summary, we have shown that THG microscopy is a powerful tool for the study of LCs. The third harmonic probe enables the investigation of molecular order well inside the LC layer. The observation of phase transition in nematic LC cells has been presented as a demonstration for the power of this technique. The method also allows direct observation of orientation fluctuations and their dynamics. We believe that this method is unique in its ability to resolve the three-dimensional structure of the LC alignment, and is therefore very promising for research of LC materials and devices.

This research was supported in part by Grants from the United States–Israel Binational Science Foundation and from the Israel Ministry of Science.

¹Y. Barad, H. Eisenberg, M. Horowitz, and Y. Silberberg, *Appl. Phys. Lett.* **70**, 922 (1997).

²J. A. Squier, M. Müller, G. J. Brakenhoff, and K. R. Wilson, *Opt. Express* **3**, 315 (1998).

³P. J. Collings and J. S. Patel, *Handbook of Liquid Crystal Research* (Oxford University Press, New York, 1996).

⁴S. Kumar, *Liquid Crystals in the Nineties and Beyond* (World Scientific, Singapore, 1995); B. Bahadur, *Liquid Crystals: Applications and Uses* (World Scientific, Singapore, 1990), Vols. I–III.

⁵D. W. Berreman, *Appl. Phys. Lett.* **25**, 12 (1974); *J. Opt. Soc. Am.* **62**, 502 (1972); **63**, 1374 (1973); *Philos. Trans. R. Soc. London, Ser. A* **309**, 203 (1983).

⁶S. C. Davey, J. Budai, J. W. Goodby, R. Pindak, and D. E. Moncton, *Phys. Rev. Lett.* **53**, 2129 (1984).

⁷R. Boyd, *Nonlinear Optics* (Academic, New York, 1992).

⁸K. Amundson, A. van Blaaderen, and P. Wiltzius, *Phys. Rev. E* **55**, 1646 (1997).

⁹G. A. Held, L. L. Kosbar, I. Dierking, A. C. Lowe, G. Grinstein, V. Lee, and R. D. Miller, *Phys. Rev. Lett.* **79**, 3443 (1997).

¹⁰P. G. De Gennes and J. Prost, *The Physics of Liquid Crystals* (Clarendon, Oxford, 1993).